ISSN 0915-633X

NATIONAL INSTITUTE FOR FUSION SCIENCE

Trapped Electron Instabilities due to Electron Temperature Gradient and Anomalous Transport

T. Yamagishi

(Received – Sep. 16, 1993)

NIFS-247 Oct. 1993

RESEARCH REPORT
NIFS Series

NAGOYA, JAPAN

Trapped Electron Instabilities due to Electron Temperature Gradient and Anomalous Transport

T.Yamagishi
Fukui Institute of Technology
Gakuen Fukui 910

Abstract

The electrostatic trapped electron instabilities have been investigated by numerically solving the local single energy integral form dispersion relation. With the electron temperature gradient, the electron collision effect destabilizes the dissipative trapped electron mode (DTEM). For collisionless electrons, the energy dependent curvature drift effect strongly destabilizes the collisionless trapped electron mode. The growth rate is, however, reduced by a small collision effect. The anomaluous transport due to these trapped electron modes is discussed.

Keywords: Electrostatic local dispersion relation for trapped electrons, single energy integral form, numerical calculation, dissipative trapped electron mode, curvature drift, electron temperature gradient, collisionless trapped electron mode, anomalous electron transport.

§1. Introduction

Trapped particle instabilities have been studied by many authors in connection with the anomalous plasma transport[1)-6)]. It is well known that the electron collision effect excites so called dissipative trapped electron mode(DTEM). In the simple model of the constant collision frequency, the collision stabilizes by the collision damping effect. The DTEM is destabilized, combined with the electron temperature gradient, when the energy dependence of the collision frequency is taken into account. This situation is similar to the η_i-mode which is excited by taking into account the energy dependence of the curvature drift frequency ω_D[7)]

In addition to the collision effect, if we take into account the energy dependent electron curvature drift effect, the trapped electron mode may be more destabilized. Due to this energy dependence, the analytical solution to the dispersion relation is at best limited to perticular asymptotic cases. For arbitrary parameter ranges, the dispersion relation may only be solved by numerical calculations.

The purpose of this report is to examine the effects of electron temperature gradient energy dependent electron collision, and curvature drift frequency for trapped electron modes by numerically solving the electrostatic local dispersion relation, and compare with usual analytical results.

We assume a simple model for ion dynamics neglecting the effects of trapped ions, finite Larmor radius, curvature drift and transit frequency. By solving the complex integral equation by a comformal mapping method, the growth rate γ is found to be much larger than expected. Due to the combined effects of the electron temperature gradient and curvature drift, γ can even be larger than the electron diamagnetic drift frequency $\omega^*{}_e$.

In actual situations, the growth rate may be smaller by various stabilizing effects such as the finite ion Larmor radius effect, transit particle effect and finite β-effect. Although our model may be too simple to be realistic, we can see, at least, what is the most important source for the trapped electron instabilities.

§2. Electrostatic Dispersion Relation

We start with the gyrokinetic solution for the perturbed ion distribution

$$\tilde{f}_i = -\frac{e\tilde{\varphi}}{T_i}\left\{1-\frac{\bar{\omega}-\omega_{*Ti}}{\bar{\omega}-\omega_{Di}}J_0(\alpha)\right\}F_{Mi} \tag{1}$$

The perturbed distribution for trapped elctrons is given by

$$\tilde{f}_e = -\frac{e\tilde{\varphi}}{T_e}\left\{1-\frac{\bar{\omega}-\omega_{*Te}}{\bar{\omega}-\omega_{De}+i\nu_{eff}}\right\}F_{Me} \tag{2}$$

where all notations are standard[7]: $\omega_D=\omega_D(v_\perp^2/2+v_\parallel^2)$, $\omega_D=2\varepsilon_n\omega^*/\tau$, $\tau=T_e/T_i$, $\varepsilon_n=L_n/L_B$, $1/L_n=-d\ln n/dr$, $1/L_B=-d\ln B/dr$ $\omega^*_T=\omega^*_e(1+\eta(v_\perp^2+v_\parallel^2-3/2))/\tau$, $\eta=d\ln T/d\ln n$, $\omega^*_e=k_y cT_e/eBL_n$, $F_M=(\pi v_{th}^2)^{-3/2}\exp(-E/T)$, and $\nu_{eff}=\nu_e/\varepsilon$ with $\varepsilon=r/R$ for tokamak, and $\varepsilon=\varepsilon_h$(helical inhomogeniety factor) for the helically symmetric system. We neglect the passing electron distribution, because it is of the order ω_*/ω_t which must be much smaller than that of trapped elctrons, where ω_t is the electron transit frequency $\omega_t=k_\parallel v_\parallel$.

If we neglect the curvature drift frequency and also finite Larmor radius effect for ion in eq.(1), the perturebed ion density is approximated by[8]:

$$\tilde{n}_i \cong \frac{\omega_{*e}}{\bar{\omega}}\frac{e\tilde{\varphi}}{T_e}N \tag{3}$$

where $\bar{\omega}=\omega+\omega_E$ with $\omega_E=v_E k_\theta$, $v_E=cE_r/B$ is the poloidal rotation velocity due to the radial electric field E_r. Integrating eq.(2) over the velocity, we have the pertubed electron density

$$\tilde{n}_e = \frac{e\tilde{\varphi}}{T_e}N\left(1-\int_T\frac{\bar{\omega}-\omega_{*Te}}{\bar{\omega}-\omega_{De}+i\nu_{eff}}F_{Me}d^3v\right) \tag{4}$$

From the quasi-neutrality condition, we have the local electrostatic dispersion relation:

$$D_{es}=1-\frac{\omega_{*e}}{\bar{\omega}}-\int_T \frac{\bar{\omega}-\omega_{*Te}}{\bar{\omega}-\omega_{De}+i\nu_{eff}} F_{Me} d^3v=0 \qquad (5)$$

The velocty integral in eq.(5) can be rewritten in the form of double integral:

$$D_{es}=1-\frac{1}{\omega}-\frac{2}{\sqrt{\pi}}\int_0^{\infty} dv_{\perp} v_{\perp} e^{-v_{\perp}^2} \int_{v_{\parallel}\le\sqrt{\varepsilon}v_{-}} dv_{\parallel} \frac{\left(\omega-1-\eta_e\left(v_{\perp}^2+v_{\parallel}^2-\frac{3}{2}\right)\right)e^{-v_{\parallel}^2}}{\omega-2\varepsilon_n\left(v_{\perp}^2/2+v_{\parallel}^2\right)+i\nu_{effo}\left(v_{\perp}^2+v_{\parallel}^2\right)^{-3/2}} \qquad (6)$$

Equation (6) may only be solved by numerical calcultions. The double intgration is, however, time consuming particulary near the resonance condition. We approximate[7] the curvature drift frequency by $\omega_D=2\varepsilon_n(v_{\perp}^2/2+v_{\parallel}^2)\cong 2\varepsilon_n(v_{\perp}^2+v_{\parallel}^2)=2\varepsilon_n E$. Equation (6) in this case can be rewritten in the form of single integral with respect to the normalized energy E:

$$D_{es}=1-\frac{1}{\omega}-\frac{2}{\sqrt{\pi}}\sqrt{\varepsilon_T}\int_0^{\infty} dE\sqrt{E}e^{-E}\frac{\omega-1-\eta_e\left(E-\frac{3}{2}\right)}{\omega-2\varepsilon_n E+i\nu_{effo}E^{-3/2}}=0 \qquad (7)$$

For the sake of simplicity, we express the normalized frequency $\bar{\omega}/\omega_{*e}$ as ω. To our trapped electron mode, the electron temperature gradient is essential. The importance of η_e can be seen by setting $\eta_e=0$ in eq.(6) or (7). In this case, these equations yield an exact solution $\omega=1$ and anothor damping branch, i.e., without electron temperature gradient all branches are stabilized.

We will solve eq.(7) numerically by making use of a conformal mapping method, i.e., by mapping certain orthognal curves in the complex ω-plane onto the complex D_{es}-plane and seek the point in the complex ω-plane until D_{es} tends to the origin in the complex D_{es}-plane.

§3. Dissipative Trapped Electron Mode

First we consider the trapped electron instability induced by the electron collision effect. If we assume the curvature drift and collision frequencies, ω_D and ν_{eff}, are respectvely constants. In this case, eq.(7) can be written by

$$1-\frac{1}{\omega}-\frac{\sqrt{\varepsilon_T}}{\omega-2\varepsilon_n+i\nu_{eff}}\left\{\left(\omega-1+\frac{3}{2}\eta_e\right)I_0-\eta_e I_1\right\}=0 \tag{8}$$

where the moment integral I_j has been defined by

$$I_j=\frac{2}{\sqrt{\pi}}\int_0^\infty dx\sqrt{x}e^{-x}x^j \tag{9}$$

Since $I_0=1$ and $I_1=3/2$, η_e term is exactly cancelled out and eq.(8) yields the solution

$$\omega=1 \quad \text{or} \quad \omega=\frac{2\varepsilon_n-i\nu_{eff}}{1-\sqrt{\varepsilon_T}} \tag{10}$$

Both eigenvalues indicate the stable branches. This means that as long as ω_D and ν_{eff} are constants, we have no instabilty.

If we introduce the energy dependence of these frequencies, the trapped particle instabilities are excited. Let us solve eq.(7) in the collisional regime: $\nu_{eff}\gg\omega_*$. Expanding the integrand in eq.(7) in powers of ω/ν_{eff}, we have

$$D_{es}=1-\frac{1}{\omega}+2i\frac{\sqrt{\varepsilon_T}}{\nu_{effo}}\left[2(\omega-1)-3\eta_e+\frac{i}{\nu_{effo}}\left\{(\omega-1+\frac{3}{2}\eta_e)(\omega I_3-2\varepsilon_n I_4)-\eta_e(\omega I_4-2\varepsilon_n I_5)\right\}\right]=0 \tag{11}$$

To the first order of ω/ν_{eff}, the solution to eq.(11) is obtained by

$$\omega=1+i\sqrt{\varepsilon_T}\frac{6\eta_e}{\sqrt{\pi}\nu_{effo}} \tag{12}$$

As compared to the usual growth rate $\gamma=\varepsilon^{3/2}\omega_*^2\eta_e/\nu_e$[1)2)] for the DTEM, the growth rate given by eq.(12) is larger by a numerical factor $6/\pi^{1/2}$. The effect of curvature drift frequency ω_D is the second order to ω/ν_{eff}, and may be negiligible in the collisional regime. In the limit, $\nu_e \to \infty$, the eigenvalue ω tends to the stable point 1. In the opposite collisionless limit, $\nu_e \to 0$, the eigenvalue ω also tends to the same stable point 1, which can be seen from eq.(10).

For arbitrary collision frequencies, eq.(7) is numerically solved by the conformal mapping method. Variation of the discrete eigenvalue for the case of $\omega_D=0$ is presented in Fig.1 for various values of ν_e and η_e. Since the eigenvalue ω tends to the same limit 1 for $\nu_e \to 0$ and $\nu_e \to \infty$, the eigenvalue trajectory for each η_e forms a closed contour. As η_e is reduced, the contour shrinks and finally tends to a stable point $\omega=1$, i.e., the electron temperature gradient is essential to the DTEM as mentioned in the above.

The normalized frequency and growth rate are also plotted versus the normalized collision frequency ν_e for different values of η_e in Fig.2. The asymptotic solution (12) presented by the broken curve is also compared in Fig.2. As seen in Figs. 1 and 2, the growth rate γ sharply increases in the weakly collisional regime, $\nu_e<1$. As ν_e increases, however, γ suffers collision damping and decreases. When the curvature drift effect is taken into account, the trapped electron mode is strongly destabilized as seen by the case of $\varepsilon_n=0.1$ in Fig.2. This branch seems to be strongly destabilized particularly in the collisionless limit.

§4. Collisionless Trapped Electron Mode

We now consider the effect of curvature drift on the trapped electron mode in the collisionless limit. In this case, eq.(7) can be rewritten in the form

$$D_{es}=1-\frac{1}{\omega}-\sqrt{\varepsilon_T}\,\frac{\eta_e}{2\varepsilon_n}-2\sqrt{\frac{\varepsilon_T}{\pi}}\left\{1-\frac{3}{2}\eta_e-\left(1-\frac{\eta_e}{2\varepsilon_n}\right)\omega\right\}\int_0^\infty\frac{\sqrt{E}e^{-E}dE}{2\varepsilon_n E-\omega} \qquad (13)$$

If we change the variable by $E=x^2$, the integral in eq.(13) can be expressed in terms of the usual plasma dispersion function Z:

$$\frac{1}{\sqrt{\pi}}\int_0^\infty \frac{\sqrt{E}e^{-E}dE}{2\varepsilon_n E-\omega}=\frac{1}{2\varepsilon_n}\left\{1+\sqrt{\frac{\omega}{2\varepsilon_n}}Z\left(\sqrt{\frac{\omega}{2\varepsilon_n}}\right)\right\} \tag{14}$$

Introducing eq.(14) into eq.(13), we have

$$D_{es}=\left(1-\sqrt{\varepsilon_T}\frac{\eta_e}{2\varepsilon_n}\right)\omega-1-\frac{\sqrt{\varepsilon_T\omega}}{\varepsilon_n}\left\{1-\frac{3}{2}\eta_e-\left(1-\frac{\eta_e}{2\varepsilon_n}\right)\omega\right\}\left\{1+\sqrt{\frac{\omega}{2\varepsilon_n}}Z\left(\sqrt{\frac{\omega}{2\varepsilon_n}}\right)\right\} \tag{15}$$

The complex function $(\omega/\omega_D)^{1/2}$ has the branch points at $\omega=0$ and at infinity. The function Z is discontinuous across the branch cut $[0,\infty]$ on the positive real axis. This branch cut corresponds to the continuous eigenvalue of the original gyrokinetic equation in the collisionless case.

When $\omega/\omega_D>>1$, applying the asymptotic formula $Z(\zeta)=-(1+1/2\zeta^2+3/4\zeta^4)/\zeta$, we find the eigenvalue $\omega=1$ in the limit $\omega_D\to 0$. Since the quantity $(\omega/\omega_D)^{1/2}$ is approximatly unity, and also the real and imaginary parts of ω are nearly the same, $\mathrm{Re}\omega\cong\mathrm{Im}\omega$, in general, we have no available asymptotic formula. Equation (15) is, therefore, not so useful to derive approximate analytical solution for the eigenvalue. We solve directly eq.(7) numerically by the conformal mapping method.

Variation of the discrete eigenvalue, the solution of eq.(7), is presented in Fig.3 for various values of η_e and ε_n. As seen in Fig.3, the normalized growth rate γ increases as η_e increases. For each η_e, as ε_n increases, the trajectory of the eigenvalue tends to the continuum, i.e., the positive real axis at which the mode becomes marginal. Figures 1 and 3 also indicate that the trapped electron modes are essentially the resonant mode at the electron diamagnetic drift frequency, $\omega=\omega_{*e}$.

Let us analytically evaluate the critical value of η_e above which the trapped particle mode becomes unstable. At the marginal state, $\gamma=0$, applying the formula: $(x+i0)^{-1}=Px^{-1}-i\pi\delta(x)$ to the integrand of eq.(13), from the real and imaginary parts, we have two equations

$$\left(1-\sqrt{\varepsilon_T}\frac{\eta_e}{2\varepsilon_n}\right)\omega-1-\sqrt{\varepsilon_T}\,\omega\left\{1-\frac{3}{2}\eta_e-\left(1-\frac{\eta_e}{2\varepsilon_n}\right)\omega\right\}\frac{2}{\sqrt{\pi}}P\int_0^\infty\frac{\sqrt{E}e^{-E}dE}{2\varepsilon_n E-\omega}=0 \qquad (16)$$

$$\left\{1-\frac{3}{2}\eta_e-\left(1-\frac{\eta_e}{2\varepsilon_n}\right)\omega\right\}\frac{1}{2\varepsilon_n}\sqrt{\frac{\omega}{2\varepsilon_n}}\exp\left(-\sqrt{\frac{\omega}{2\varepsilon_n}}\right)=0 \qquad (17)$$

From eq.(17), we have $\omega=(1-3\eta_e/2)/(1-\eta_e/\omega_D)$. Introducing this relation into eq.(16), we have $\omega=\omega_D/(\omega_D-\varepsilon^{1/2}\eta_e)$ and the relation between η_e and ε_n in the form

$$\varepsilon_n=\frac{1}{3}\left(1-\sqrt{\varepsilon_T}+\frac{3}{2}\sqrt{\varepsilon_T}\eta_e\right) \qquad (18)$$

In the derivation of eq.(18), we assumes no approximation, i.e., the critical condition (18) is exact. The boundary in the (ε_n,η_e)-plane given by eq.(18) is shown in Fig.4. The evaluation of the critical value by numerical method has the difficulty due to the singularity. The numerical integration for the singular function must be very careful. The boundary values obtained by numerical calculations are close to the curve shown in Fig.4. For the collisionless case, the unstable region below the line given by Eq.(18) is limited in the region $\varepsilon_n>0$.

The critical boudary curve is also calculated numerically for the case with the collision effect. As seen in Fig.4, when the collision effect$(\hat{\nu}_e=1)$ is introduced, the stable region in the (η_e,ε_n)-plane is enlarged. How the collision effect stabilizes the trapped electron mode can also be seen by the eigenvalue shown by the dotted curve in Fig. 3. As compared with the eigenvalue of $\eta_e=1$, the dotted trajectory with the collision effect, $\hat{\nu}_e=1$, is much reduced.

The weak collision effect exites the DTEM. On the other hand, the same weak collision effect strongly stabilizes the collisionless trapped electron mode induced by the curvature drift. This situation can be seen in Fig.5, where the normalized growth rates for $\varepsilon_n=0$ (DTEM) and $\varepsilon_n=0.2$ are plotted versus $\hat{\nu}_e$ for comparison.

§5. Anomalous Electron Diffusion

We proceed to the derivation of electron diffusion coefficient induced by the trapped electron modes. Let us consider the cross field quasi-linear electron flux

$$\Gamma_e = \int d^3v \langle \tilde{v}_x \tilde{f}_e \rangle \tag{19}$$

where the angular brackets means the ensemble average. Introducing Fourier representation of $\tilde{v}_x = ick_\theta\tilde{\phi}/B$ and eq.(2) into eq.(19), we have

$$\Gamma_e = \sum \left|\frac{e\tilde{\varphi}}{T_e}\right|^2_{k\omega} \frac{cT_e}{eB} k_\theta \mathrm{Im}\left(\int d^3v \frac{\bar{\omega}-\omega_{*Te}}{\bar{\omega}-\omega_{De}+i\nu_{eff}} F_{Me}\right) \tag{20}$$

The flux due to the discrete trapped electron modes must be evaluated by introducing the discrete eigenvalue $\omega=\omega_r+i\gamma$ given by the dispersion relation (5). From eq.(5), the imaginary part of the integral in eq.(20) can be expressed by the discrete eigenvalue in the form[9]

$$\mathrm{Im}\left(\int d^3v \frac{\bar{\omega}-\omega_{*Te}}{\bar{\omega}-\omega_{De}+i\nu_{eff}} F_{Me}\right) = \frac{\omega_{*e}\gamma}{\bar{\omega}_r^2+\gamma^2} \tag{21}$$

which is exact for arbitrary ω_D and ν_{eff}.

If we apply the mixing length assumption: $|e\tilde{\phi}/T_e|^2 \approx (k_\perp L_n)^{-2}$ in eq.(20), and bearing in mind the relation: $\Gamma=-D_\perp dn/dr$, we have the electron diffusion coefficient from eqs.(20) and (21)

$$D_\perp = \frac{\omega_{*e}}{k_\perp^2} \frac{\omega_{*e}\gamma}{\bar{\omega}_r^2+\gamma^2} \tag{22}$$

When $\omega_r \approx \omega_*$ and $\gamma \ll \omega_*$, eq.(22) reduces to the usual result

$$D_\perp = \frac{\gamma}{k_\perp^2} \tag{23}$$

As we have seen in Fig.3, this assumption does not hold in general, i.e., the usual formula (23) is valid only in the limited parameter region. As seen in Fig.3, when $\eta_e>1$, and $\varepsilon_n=0.1$, the magnitude of the growth rate γ becomes nearly the same as that of the real frequency, and the assumption $\gamma \ll \omega_*$ is broken down.

As long as the test particle diffusion model and the mixing length ansatz are applied, the diffusion coefficeient due to the continuum contribution has been obtained in the similar form[9].

For the DTEM, applying the growth rate given by eq.(12) to eq.(23), we have

$$D_\perp \approx \frac{6}{\sqrt{\pi}} \frac{\varepsilon^{\frac{3}{2}} \omega_{*e}^{2} \eta_e}{\nu_e k_\perp^2} \tag{24}$$

If we introduce the gryro-Bohm coefficient by

$$D_{GB} = \frac{\rho_i^2 v_i}{L_B} \tag{25}$$

for $k \approx k_\theta$, eq.(24) can be rewitten in the form

$$D_\perp = D_{GB} \frac{6\sqrt{\varepsilon}\tau^2 v_i}{\sqrt{\pi}\varepsilon_n L_T \nu_e} \tag{26}$$

The diffusion coefficient (24) has the scaling: $D \propto T^{7/2}\varepsilon^{3/2}B^{-2}n^{-1}/L_n L_T$, i.e., D has a strong temperature dependence.

If we assume $k\,\rho_i \approx$constant as experimentally observed[10], eq.(22) can also by expressed in terms of D_{GB} :

$$D_\perp = D_{GB} \frac{\omega_{*e}\gamma}{\bar{\omega}_r^2 + \gamma^2} \frac{\tau}{\varepsilon_n} \tag{27}$$

For the collisionless plasma, the diffusion coefficient $D_\perp$ normalized by D_{GB} is plotted versus ε_n in Fig.6. As seen in Fig.6, the quantity $D_\perp/D_{GB}$ increses as η_e increases, and is sharply peaked at $\varepsilon_n \approx 0.05$ which is due to the behavior of the growth rate γ versus ε_n.

As shown in Refs.(1) and (2), and eq.(24), the asymptotic formula for the growth rate for the DTEM is proportional to the factor η_e. The importance of the electron temperature gradient effect η_e has also been seen in the numerical results in Figs.1 and 3, i.e., without η_e the trapped electron instability disappears. Recently the diffusion coefficient induced by the DTEM without the η_e-effect has been employed, among many other models, for interpretations of experimental observations[11][12]. Since the electron temperature gradient is an essential source for the trapped electron instability as pointed out in the above, the effect of η_e should be taken into account.

§6. Conclusion

Neglecting the finite Larmor radius effect and transit frequency for ions, the trapped electron instabilities induced by the electron temperature gradient have been investigated by numerically calculating the electrostatic local dispersion relation. In our model, the negative electron temperature gradient is essential to excites the dissipative and collisionless trapped electron modes. When $\eta_e=0$, all these instabilities are stabilized. Even when $\eta_e \neq 0$, if the collision frequency and curvature drift frequency are independent of velocity, the trapped electron modes are stable, as in the case of η_i-mode. The DTEM is, therefore, becomes unstable when $\eta_e \neq 0$ and ν_{eff} is velocity dependent. In the highly collisional regime, $\nu_e \gg \omega_*$, the asymptotic formula for the growth rate agrees with the numerical results calculated by a conformal mapping method.

In the collisionless regime, the combination of electron temperature gradient and curvature drift effects make the trapped electron mode strongly unstable. The frequency ω_r is positive, i.e., in the electron diamagnetic drift direction, and $\omega_r \approx \omega_*$. The growth rate γ also becomes comparable to or even larger than the electron drift frequency ω_*, i.e., γ is even larger than that of the η_i-mode. In this regime, $\omega_r \approx \gamma \approx \omega_*$, the asymptotic expansion formula for the plasma dispersion function is not available, and we have no analytical expression for the dispersion relation. In the limit, $\gamma \to 0$, of the marginal state, however, the exact analytical expression as given by eq.(18) for the stability boundary has been obtained in the collisionless case. The collision effect destabilizes the TEM in the small η_e regime, while it stabilizes the TEM in the larger η_e regime as seen in Fig.4.

The cross field electron flux which is induced by the discrete TEM has been calculated consistently with the dispersion relation, and the diffusion coefficient has been evaluated in term of the gyro-Bohm coefficient as given by eq.(24). The electron diffusion coefficient normalized by D_{GB} increases as η_e increases, and is sharply peaked at $\varepsilon_n \approx 0.1$ as ε_n varies. At the peak value $D_\perp$ is much larger than D_{GB} as shown in Fig.6.

In this study a simple model has been employed to see what is the important source of the trapped electron instabilty. If we introduce more detail of ion dynamics such as the finite Larmor radius effect, the growth rate of the TEM may be reduced[13].

Acknowledgement

The author would like to thank to Dr. H.Sanuki and Dr. M.Azumi for providing valuable information. This study is a joint research effort with the National Institute for Fusion Science.

References

(1)B.B.Kadomtsev,O.P.Pogutse, Nucl.Fusion,**11**(1971)67.

(2)W.M.Manheimer,*An Introduction to Trapped-Particle Instability in Tokamaks*, TID-27157,US-ERDA Technical Information Center (1977).

(3)S.M.Mahajan, Report IFSR#31(1981).

(4)B.Coppi and G.Rewoldt, Physics Letters, **54A**(1975)301.

(5)S.M.Mahajan and D.W.Ross,Phys.Fluids,**22**(1978)669.

(6)K.T.Tsang and P.J.Catto, Phys. Rev. Lett., **39**(1977)1664.

(7)T.Yamagishi, *Cross Field Energy Flux due to Ion Temperature Gradient Mode in a Tokamak*, US-Japan Workshop on η_i-mode and turbulent transport, University of Texas, 1993.

(8)K.Miyamoto, *Plasma Physics for Fusion*, Iwanami,Tokyo,1976.

(9)T.Yamagishi, Report NIFS-227(1993).

(10)A.J.Wooton,H.Y.Tsui and S.Prager,Plasma Physics and Cont. Fusion,**34**(1992)2023.

(11)K.Yamazaki,T.Amano,Nucl.Fusion **32**(1992)633.

(12)H.Shirai, T.Hirayama, Y.Koide, M.Azumi, D.R. Mikelsen,S.D.Scott, Ion Temperature Profile Simulation of JT-60 and TFTR Plasmas with Ion Temperature Gradient Mode, submitted to Nucl. Fusion.

(13)A.Hirose and S.G.Tsotsonis, Nucl.Fusion,**30**(1990)2063.

Figures Captions

Fig.1: Variation of normalized discrete time eigenvalue for various values of $\hat{\nu}_e=\nu_e/\omega_*$ and η_e in the complex ω-plane.

Fig.2: Variations of normalized frequency and growth rate for dissipative trapped electron mode vursus normalized collision frequency $\hat{\nu}_e$ for $\eta_e=1$.

Fig.3: Variation of normalized discrete eigenvalue for collisionless trapped electron mode for various values of ε_n and η_e. The discrete eigenvalue for DTEM is presented by the broken curve for comparison.

Fig.4: Critical boundary curves for $\hat{\nu}_e=0$ and $\hat{\nu}_e=1$ in (η_e,ε_n)-plane.

Fig.5: Comparison of normalizes growth rates for $\varepsilon_n=0$ (DTEM) and $\varepsilon_n=0.2$ as functions of normalized collision frequency $\hat{\nu}_e$.

Fig.6: Variation of electron diffusion coefficient normalized by gyroBohm coefficient versus ε_n for various values of η_e for collisionless plasma.

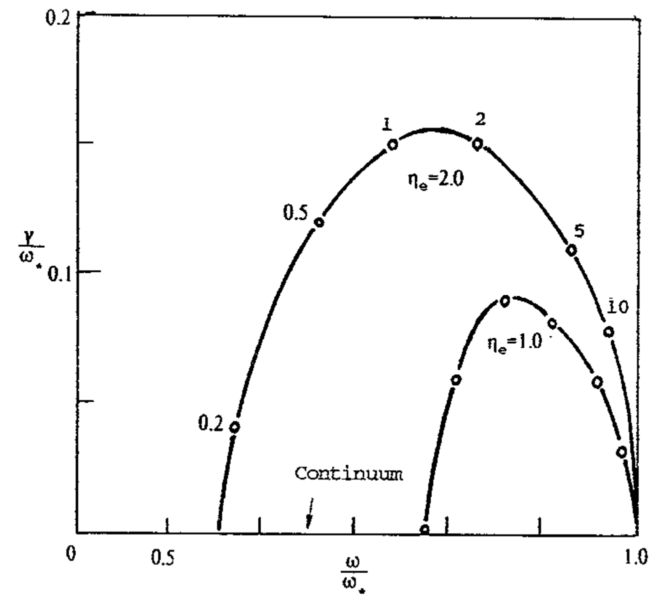
0.2
0.1
$\frac{\gamma}{\omega_*}$
1
2
0.5
η_e=2.0
5
10
η_e=1.0
0.2
Continuum
0
0.5
1.0
$\frac{\omega}{\omega_*}$

Fig.1

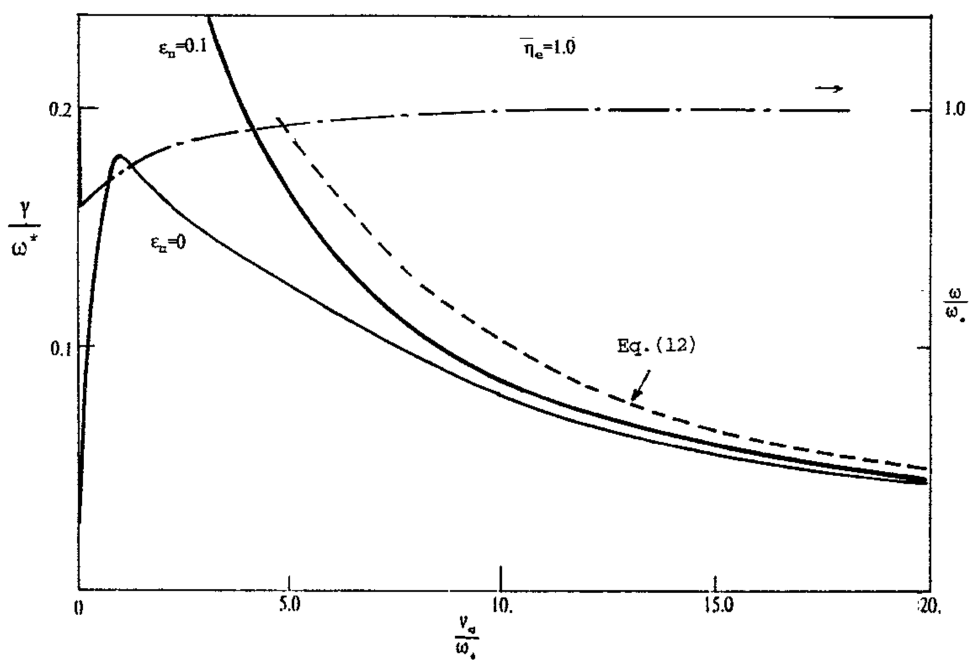
ε_n=0.1
η_e=1.0
0.2
1.0
$\frac{\gamma}{\omega^*}$
ε_n=0
$\frac{\omega}{\omega_*}$
0.1
Eq.(12)
0
5.0
10.
15.0
20.
$\frac{\nu_a}{\omega_*}$

Fig.2

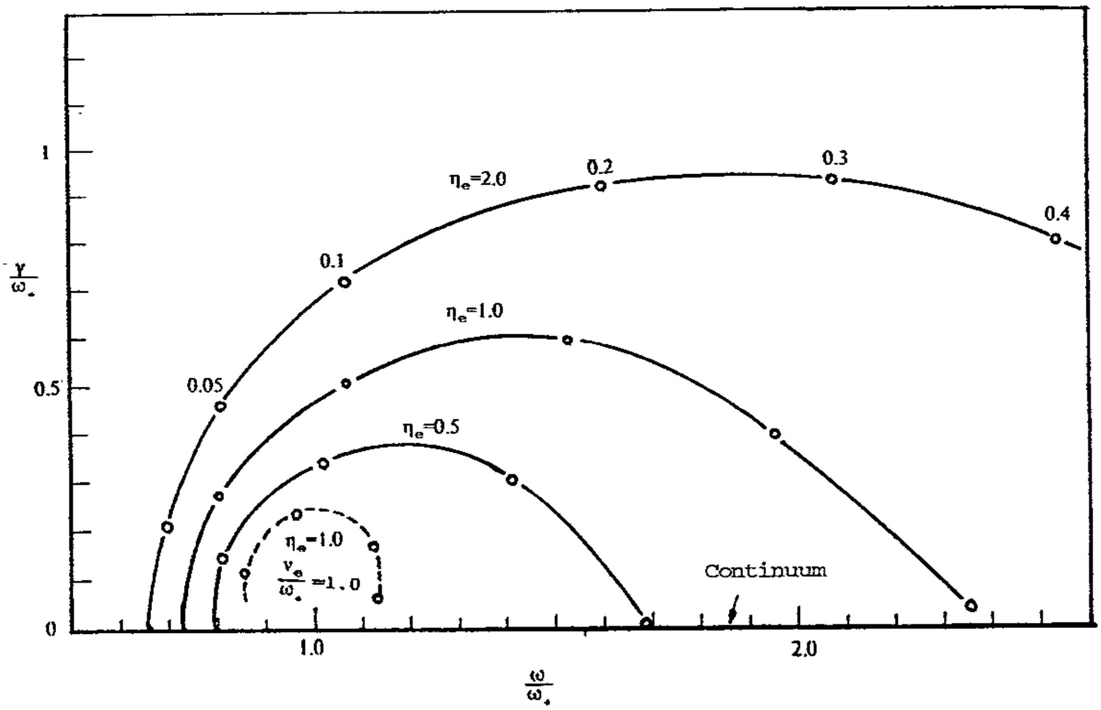

1
0.5
0
$-\frac{\gamma}{\omega_*}$
1.0
2.0
$\frac{\omega}{\omega_*}$
η_e=2.0
0.05
0.1
0.2
0.3
0.4
η_e=1.0
η_e=0.5
η_e=1.0
$\frac{\nu_e}{\omega_*}$=1.0
Continuum

Fig. 3

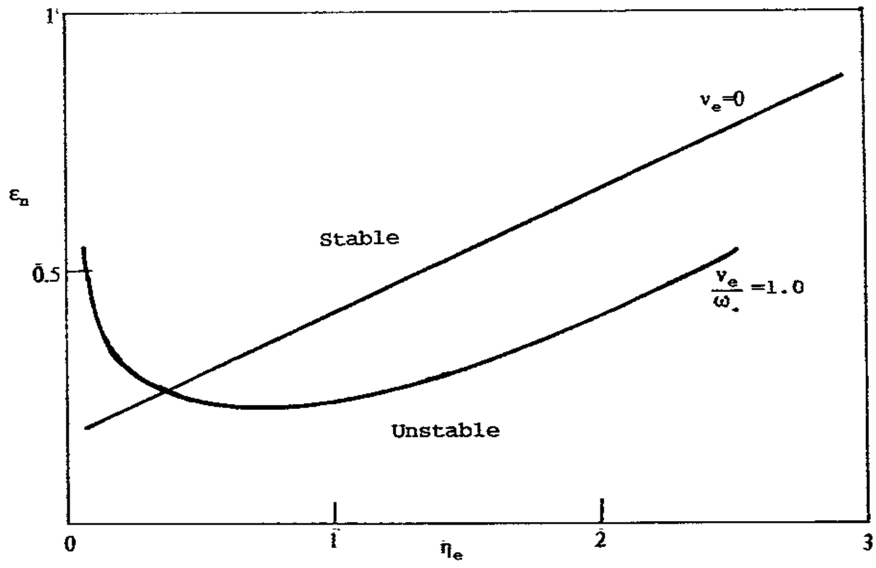

1
0.5
0
1
2
3
ε_n
η_e
ν_e=0
$\frac{\nu_e}{\omega_*}$=1.0
Stable
Unstable

Fig. 4

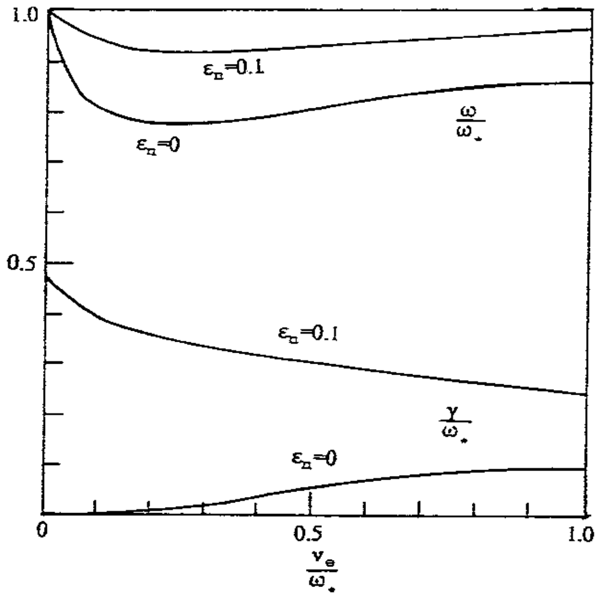

1.0
0.5
0
0.5
1.0
ε_n=0.1
ε_n=0
$\frac{\omega}{\omega_*}$
ε_n=0.1
$\frac{\gamma}{\omega_*}$
ε_n=0
$\frac{\nu_e}{\omega_*}$

Fig.5

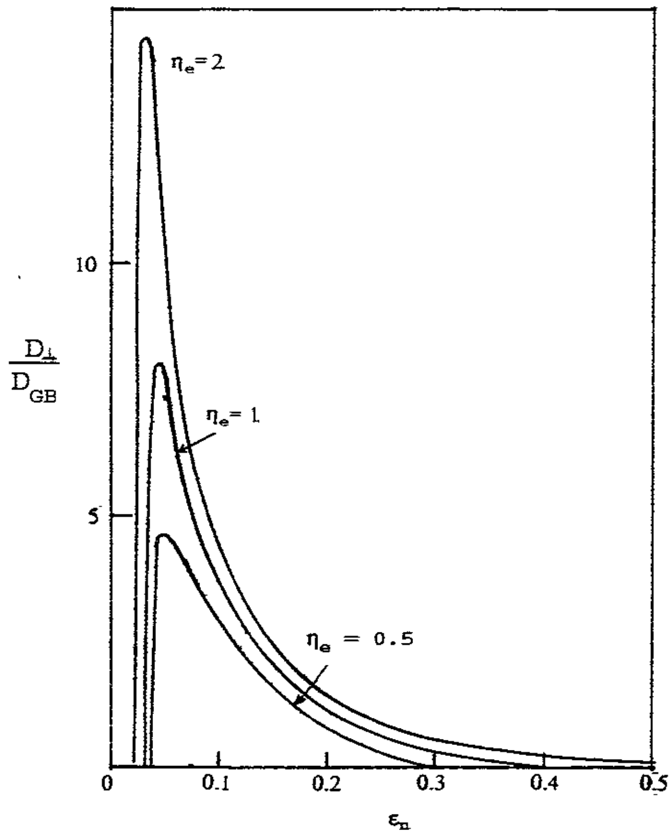

η_e= 2
10
$\frac{D_\perp}{D_{GB}}$
η_e= 1
5
η_e = 0.5
0
0.1
0.2
0.3
0.4
0.5
ε_n

Fig.6

Recent Issues of NIFS Series

NIFS-193 T. Watari, *Review of Japanese Results on Heating and Current Drive* ; Oct. 1992

NIFS-194 Y. Kondoh, *Eigenfunction for Dissipative Dynamics Operator and Attractor of Dissipative Structure* ; Oct. 1992

NIFS-195 T. Watanabe, H. Oya, K. Watanabe and T. Sato, *Comprehensive Simulation Study on Local and Global Development of Auroral Arcs and Field-Aligned Potentials* ; Oct. 1992

NIFS-196 T. Mori, K. Akaishi, Y. Kubota, O. Motojima, M. Mushiaki, Y. Funato and Y. Hanaoka, *Pumping Experiment of Water on B and LaB_6 Films with Electron Beam Evaporator* ; Oct., 1992

NIFS-197 T. Kato and K. Masai, *X-ray Spectra from Hinotori Satellite and Suprathermal Electrons* ; Oct. 1992

NIFS-198 K. Toi, S. Okamura, H. Iguchi, H. Yamada, S. Morita, S. Sakakibara, K. Ida, K. Nishimura, K. Matsuoka, R. Akiyama, H. Arimoto, M. Fujiwara, M. Hosokawa, H. Idei, O. Kaneko, S. Kubo, A. Sagara, C. Takahashi, Y. Takeiri, Y. Takita, K. Tsumori, I. Yamada and H. Zushi, *Formation of H-mode Like Transport Barrier in the CHS Heliotron / Torsatron* ; Oct. 1992

NIFS-199 M. Tanaka, *A Kinetic Simulation of Low-Frequency Electromagnetic Phenomena in Inhomogeneous Plasmas of Three-Dimensions* ; Nov. 1992

NIFS-200 K. Itoh, S.-I. Itoh, H. Sanuki and A. Fukuyama, *Roles of Electric Field on Toroidal Magnetic Confinement*, Nov. 1992

NIFS-201 G. Gnudi and T. Hatori, *Hamiltonian for the Toroidal Helical Magnetic Field Lines in the Vacuum*; Nov. 1992

NIFS-202 K. Itoh, S.-I. Itoh and A. Fukuyama, *Physics of Transport Phenomena in Magnetic Confinement Plasmas*; Dec. 1992

NIFS-203 Y. Hamada, Y. Kawasumi, H. Iguchi, A. Fujisawa, Y. Abe and M. Takahashi, *Mesh Effect in a Parallel Plate Analyzer*; Dec. 1992

NIFS-204 T. Okada and H. Tazawa, *Two-Stream Instability for a Light Ion Beam -Plasma System with External Magnetic Field;* Dec. 1992

NIFS-205 M. Osakabe, S. Itoh, Y. Gotoh, M. Sasao and J. Fujita, *A Compact Neutron Counter Telescope with Thick Radiator (Cotetra) for Fusion*

Experiment; Jan. 1993

NIFS-206 T. Yabe and F. Xiao, *Tracking Sharp Interface of Two Fluids by the CIP (Cubic-Interpolated Propagation) Scheme*, Jan. 1993

NIFS-207 A. Kageyama, K. Watanabe and T. Sato, *Simulation Study of MHD Dynamo : Convection in a Rotating Spherical Shell*; Feb. 1993

NIFS-208 M. Okamoto and S. Murakami, *Plasma Heating in Toroidal Systems*; Feb. 1993

NIFS-209 K. Masai, *Density Dependence of Line Intensities and Application to Plasma Diagnostics*; Feb. 1993

NIFS-210 K. Ohkubo, M. Hosokawa, S. Kubo, M. Sato, Y. Takita and T. Kuroda, *R&D of Transmission Lines for ECH System* ; Feb. 1993

NIFS-211 A. A. Shishkin, K. Y. Watanabe, K. Yamazaki, O. Motojima, D. L. Grekov, M. S. Smirnova and A. V. Zolotukhin, *Some Features of Particle Orbit Behavior in LHD Configurations*; Mar. 1993

NIFS-212 Y. Kondoh, Y. Hosaka and J.-L. Liang, *Demonstration for Novel Self-organization Theory by Three-Dimensional Magnetohydrodynamic Simulation*; Mar. 1993

NIFS-213 K. Itoh, H. Sanuki and S.-I. Itoh, *Thermal and Electric Oscillation Driven by Orbit Loss in Helical Systems*; Mar. 1993

NIFS-214 T. Yamagishi, *Effect of Continuous Eigenvalue Spectrum on Plasma Transport in Toroidal Systems*; Mar. 1993

NIFS-215 K. Ida, K. Itoh, S.-I.Itoh, Y. Miura, JFT-2M Group and A. Fukuyama, *Thickness of the Layer of Strong Radial Electric Field in JFT-2M H-mode Plasmas*; Apr. 1993

NIFS-216 M. Yagi, K. Itoh, S.-I. Itoh, A. Fukuyama and M. Azumi, *Analysis of Current Diffusive Ballooning Mode*; Apr. 1993

NIFS-217 J. Guasp, K. Yamazaki and O. Motojima, *Particle Orbit Analysis for LHD Helical Axis Configurations* ; Apr. 1993

NIFS-218 T. Yabe, T. Ito and M. Okazaki, *Holography Machine HORN-1 for Computer-aided Retrieve of Virtual Three-dimensional Image* ; Apr. 1993

NIFS-219 K. Itoh, S.-I. Itoh, A. Fukuyama, M. Yagi and M. Azumi, *Self-sustained Turbulence and L-Mode Confinement in Toroidal Plasmas* ; Apr. 1993

NIFS-220 T. Watari, R. Kumazawa, T. Mutoh, T. Seki, K. Nishimura and F. Shimpo, *Applications of Non-resonant RF Forces to Improvement of Tokamak Reactor Performances Part I: Application of Ponderomotive Force* ; May 1993

NIFS-221 S.-I. Itoh, K. Itoh, and A. Fukuyama, *ELMy-H mode as Limit Cycle and Transient Responses of H-modes in Tokamaks* ; May 1993

NIFS-222 H. Hojo, M. Inutake, M. Ichimura, R. Katsumata and T. Watanabe, *Interchange Stability Criteria for Anisotropic Central-Cell Plasmas in the Tandem Mirror GAMMA 10 ;* May 1993

NIFS-223 K. Itoh, S.-I. Itoh, M. Yagi, A. Fukuyama and M. Azumi, *Theory of Pseudo-Classical Confinement and Transmutation to L-Mode;* May 1993

NIFS-224 M. Tanaka, *HIDENEK: An Implicit Particle Simulation of Kinetic-MHD Phenomena in Three-Dimensional Plasmas;* May 1993

NIFS-225 H. Hojo and T. Hatori, *Bounce Resonance Heating and Transport in a Magnetic Mirror;* May 1993

NIFS-226 S.-I. Iton, K. Itoh, A. Fukuyama, M. Yagi, *Theory of Anomalous Transport in H-Mode Plasmas;* May 1993

NIFS-227 T. Yamagishi, *Anomalous Cross Field Flux in CHS ;* May 1993

NIFS-228 Y. Ohkouchi, S. Sasaki, S. Takamura, T. Kato, *Effective Emission and Ionization Rate Coefficients of Atomic Carbons in Plasmas;* June 1993

NIFS-229 K. Itoh, M. Yagi, A. Fukuyama, S.-I. Itoh and M. Azumi, *Comment on 'A Mean Field Ohm's Law for Collisionless Plasmas;* June 1993

NIFS-230 H. Idei, K. Ida, H. Sanuki, H. Yamada, H. Iguchi, S. Kubo, R. Akiyama, H. Arimoto, M. Fujiwara, M. Hosokawa, K. Matsuoka, S. Morita, K. Nishimura, K. Ohkubo, S. Okamura, S. Sakakibara, C. Takahashi, Y. Takita, K. Tsumori and I. Yamada, *Transition of Radial Electric Field by Electron Cyclotron Heating in Stellarator Plasmas;* June 1993

NIFS-231 H.J. Gardner and K. Ichiguchi, *Free-Boundary Equilibrium Studies for the Large Helical Device,* June 1993

NIFS-232 K. Itoh, S.-I. Itoh, A. Fukuyama, H. Sanuki and M. Yagi, *Confinement Improvement in H-Mode-Like Plasmas in Helical Systems,* June 1993

NIFS-233 R. Horiuchi and T. Sato, *Collisionless Driven Magnetic Reconnection,* June 1993

NIFS-234 K. Itoh, S.-I. Itoh, A. Fukuyama, M. Yagi and M. *Azumi, Prandtl Number of Toroidal Plasmas;* June 1993

NIFS-235 S. Kawata, S. Kato and S. Kiyokawa , *Screening Constants for Plasma;* June 1993

NIFS-236 A. Fujisawa and Y. Hamada, *Theoretical Study of Cylindrical Energy Analyzers for MeV Range Heavy Ion Beam Probes;* July 1993

NIFS-237 N. Ohyabu, A. Sagara, T. Ono, T. Kawamura and O. Motojima, *Carbon Sheet Pumping;* July 1993

NIFS-238 K. Watanabe, T. Sato and Y. Nakayama, *Q-profile Flattening due to Nonlinear Development of Resistive Kink Mode and Ensuing Fast Crash in Sawtooth Oscillations;* July 1993

NIFS-239 N. Ohyabu, T. Watanabe, Hantao Ji, H. Akao, T. Ono, T. Kawamura, K. Yamazaki, K. Akaishi, N. Inoue, A. Komori, Y. Kubota, N. Noda, A. Sagara, H. Suzuki, O. Motojima, M. Fujiwara, A. Iiyoshi, *LHD Helical Divertor;* July 1993

NIFS-240 Y. Miura, F. Okano, N. Suzuki, M. Mori, K. Hoshino, H. Maeda, T. Takizuka, JFT-2M Group, K. Itoh and S.-I. Itoh, *Ion Heat Pulse after Sawtooth Crash in the JFT-2M Tokamak;* Aug. 1993

NIFS-241 K. Ida, Y.Miura, T. Matsuda, K. Itoh and JFT-2M Group, *Observation of non Diffusive Term of Toroidal Momentum Transport in the JFT-2M Tokamak;* Aug. 1993

NIFS-242 O.J.W.F. Kardaun, S.-I. Itoh, K. Itoh and J.W.P.F. Kardaun, *Discriminant Analysis to Predict the Occurrence of ELMS in H-Mode Discharges;* Aug. 1993

NIFS-243 K. Itoh, S.-I. Itoh, A. Fukuyama, *Modelling of Transport Phenomena;* Sep. 1993

NIFS-244 J. Todoroki, *Averaged Resistive MHD Equations;* Sep. 1993

NIFS-245 M. Tanaka, *The Origin of Collisionless Dissipation in Magnetic Reconnection;* Sep. 1993

NIFS-246 M. Yagi, K. Itoh, S.-I. Itoh, A. Fukuyama and M. Azumi, *Current Diffusive Ballooning Mode in Seecond Stability Region of Tokamaks;* Sep. 1993